Translating aboveground cosmic-ray neutron intensity to high-frequency soil moisture profiles at sub-kilometer scale

R. Rosolem[1], T. Hoar[2], A. Arellano[3], J. L. Anderson[2], W. J. Shuttleworth[4], X. Zeng[3], and T. E. Franz[5]

[1]Queens School of Engineering, University of Bristol, Bristol, UK
[2]NCAR Data Assimilation Research Section, Boulder, USA
[3]Department of Atmospheric Sciences, University of Arizona, Tucson, USA
[4]Department of Hydrology and Water Resources, University of Arizona, Tucson, USA
[5]School of Natural Resources, University of Nebraska-Lincoln, Lincoln, USA

Correspondence to: R. Rosolem (rafael.rosolem@bristol.ac.uk)

Abstract. Above-ground cosmic-ray neutron measurements provide an opportunity to infer soil moisture at the sub-kilometer scale. Initial efforts to assimilate those measurements have shown promise. This study expands such analysis by investigating (1) how the information from aboveground cosmic-ray neutrons can constrain the soil moisture at distinct depths simulated by a land surface model, and (2) how changes in data availability (in terms of retrieval frequency) impact the dynamics of simulated soil moisture profiles. We employ ensemble data assimilation techniques in a "nearly-identical twin" experiment applied at semi-arid shrubland, rainfed agricultural field, and mixed forest biomes in the USA. The performance of the Noah land surface model is compared with and without assimilation of observations at hourly intervals, as well as every 2 days. Synthetic observations of aboveground cosmic-ray neutrons better constrain the soil moisture simulated by Noah in root-zone soil layers (0–100 cm), despite the limited measurement depth of the sensor (estimated to be 12–20 cm). The ability of Noah to reproduce a "true" soil moisture profile is remarkably good, regardless of the frequency of observations at the semi-arid site. However, soil moisture profiles are better constrained when assimilating synthetic cosmic-ray neutron observations hourly rather than every 2 days at the cropland and mixed forest sites. This indicates potential benefits for hydrometeorological modeling when soil moisture measurements are available at a relatively high frequency. Moreover, differences in summertime meteorological forcing between the semi-arid site and the other two sites may indicate a possible control-

ling factor to soil moisture dynamics in addition to differences in soil and vegetation properties.

1 Introduction

The water stored in soils controls the hydrometeorology of a region by partitioning the rainfall into surface runoff and infiltration. In addition, soil water controls the amount of available energy used for water vapor exchanges with the atmosphere, as opposed to sensible or ground heat exchange. Soil moisture can also potentially impact biogeochemical interactions between land and atmosphere. With the increased frequency of relevant hydrometeorological events (Coumou and Rahmstorf, 2012; IPCC, 2012), such as floods and droughts, a more accurate representation of the soil water is needed for improved weather and climate predictions and for better practices in agriculture and water resources planning (Koster et al., 2004; Seneviratne, 2012).

In weather and climate models, the exchanges of water, heat, and momentum between land and atmosphere are simulated by so-called land surface models (LSMs). Such models have evolved over the last few decades (Best et al., 2011; Bonan et al., 2002; Clark et al., 2011; Niu et al., 2011; Oleson et al., 2008; Pitman, 2003; Sellers et al., 1997; Yang et al., 2011), in part due to comparison studies using flux tower measurements (e.g., Baker et al., 2008, 2003; Rosolem et al., 2012a, b; Sakaguchi et al., 2011; Sellers et al., 1989; Wang et al., 2010), such as the AmeriFlux network (Baldocchi, 2003).

However, until recently, soil moisture measurements at spatial scales comparable to the horizontal footprint of flux towers and grid sizes employed in LSMs (Wood et al., 2011) had been difficult and costly (Robinson et al., 2008).

Traditional point-scale soil moisture measurements are usually available at high frequency (e.g., hourly), but suffer from having a small support volume (a few tens of centimeters). On the other hand, large-scale soil moisture measurements are available globally through satellite remote sensing (Brown et al., 2013; Entekhabi et al., 2010; Kerr et al., 2010), but have low-frequency retrievals (1–3 days) and shallow penetration depths (1–5 cm). This potentially limits knowledge of the root-zone soil moisture that provides the link between land and atmosphere via evapotranspiration (Seneviratne et al., 2010).

Recent innovative technology provides an opportunity to estimate soil moisture at scales comparable to flux tower footprints using cosmic rays (Zreda et al., 2008). The measurement relies on the natural production of fast (low-energy) neutrons in the soil from high-energy neutrons created by cosmic rays. This process is strongly controlled by the much higher absorbing/moderating power of hydrogen atoms relative to other chemical elements (see Fig. 5 in Zreda et al., 2012). Therefore, when soil is relatively wet with high hydrogen content, fewer fast neutrons reach the surface than when the soil is dry with low hydrogen content. The cosmic-ray sensor measures the neutron intensity (referred to as moderated neutrons count over a given period of time – usually an hour), which is consequently related to the soil water content. The horizontal effective measurement area is near-constant and approximately 300 m in radius at sea level under a dry atmosphere (Desilets and Zreda, 2013), while the effective measurement depth varies approximately from 10 to 70 cm, depending on the total soil water (i.e., pore plus chemically bound "lattice" water, as discussed in Franz et al., 2012a), see Fig. 1. This new technology is being investigated around the globe in newly established networks, such as the COsmic-ray Soil-Moisture Observing System in the USA (COSMOS; http://cosmos.hwr.arizona.edu) (Zreda et al., 2012), the Australian National Cosmic Ray Soil-Moisture Monitoring Facility (CosmOz; http://www.ermt.csiro.au/html/cosmoz.html) (Hawdon et al., 2014), the German Terrestrial Environmental Observatories (TERENO; http://teodoor.icg.kfa-juelich.de/overview-en) (Zacharias et al., 2011), and most recently in Africa (http://cosmos.hwr.arizona.edu/Probes/africa.php) and the UK (COSMOS-UK; http://www.ceh.ac.uk/cosmos).

Initial efforts to assimilate near surface cosmic-ray neutrons into hydrometeorological models have shown promising results (Shuttleworth et al., 2013; Han et al., 2014), but focused mainly on the signal associated with the integrated, depth-weighted soil moisture estimates. The present study expands the application of the cosmic-ray soil moisture using ensemble data assimilation techniques. The objectives here are:
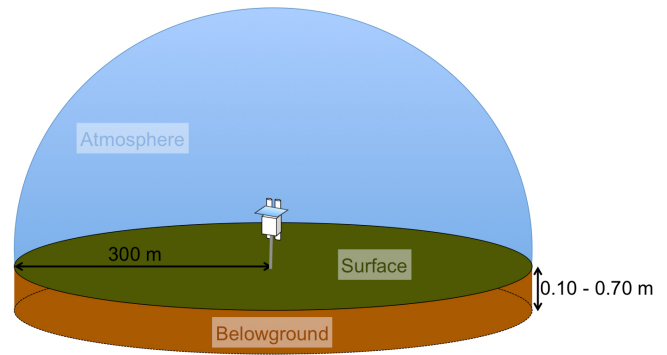

Figure 1. Schematic representation of the effective measurement volume for the cosmic-ray soil moisture sensor. The effective depth depicted in the figure refers to the overall range in the sensor (Zreda et al., 2008). Notice that the effective depth estimated for the synthetic experiments in this study varies approximately between 12 and 20 cm (refer to text).

1. to determine how effectively the information from aboveground cosmic-ray neutrons is propagated to individual soil moisture layers in a land surface model;

2. to assess the benefits/limitations of high-frequency retrieval offered by this new technology.

Analyses are carried out for the summer period (May through September 2012) at three distinct biomes in the USA using synthetic observations of neutron intensity obtained from the LSM.

2 Data and methods

2.1 Sites description

Site selection was made based on the availability of meteorological forcing data from the AmeriFlux network (http://ameriflux.lbl.gov), and to include characteristic differences in site-to-site climatology, land cover and soil types, as summarized in Table 1. The soil and vegetation types at each site were assigned the following classifications obtained from the AmeriFlux database. The Kendall site located in the Walnut Gulch Experimental Watershed is a semi-arid grassland comprising mainly of C4 grasses with a few scattered shrubs with a dominant growing season in response to the summer rains (Scott et al., 2010). The Nebraska site, located at the University of Nebraska Agricultural Research and Development Center, is a rainfed agricultural field characterized by maize-soybean rotation with a growth period (planting to harvest) from May to October (Verma et al., 2005). The Park Falls/WLEF tower located in the Park Falls Ranger District of the Chequamegon National Forest is characterized by a managed landscape, where logging activities, such as thinning and clear-cuts, are concentrated in the upland region (Davis et al., 2003). The growing seasons are typically short

Table 1. Site information obtained from AmeriFlux database (http://ameriflux.lbl.gov). MAT = mean annual temperature, and MAP = mean annual precipitation. Notice the analyzed period in this study is a subset of the available data from each site and it is defined from 1 May 2012, 00:00 UTC to 30 September 2012, 23:00 UTC.

Site	Latitude	Longitude	Land cover	Soil type	MAT (°C)	MAP (cm)	Spin-up period (one cycle)
Kendall	31°74′ N	109°94′ W	Grasslands	Loam	16	41	1 January 2010, 00:00 UTC to 31 December 2012, 23:00 UTC
Nebraska	41°10′ N	96°26′ W	Croplands	Silty clay loam	10	78	1 January 2011, 00:00 UTC to 31 December 2012, 23:00 UTC
Park Falls	45°56′ N	90°16′ W	Mixed forest	Sandy loam	4	82	1 January 2011, 00:00 UTC to 31 December 2012, 23:00 UTC

and the winters long and cold (Mackay et al., 2002). Soil moisture availability controls summer evapotranspiration at the Kendall and Nebraska sites and, to a lesser extent, at the Park Falls (Teuling et al., 2009).

In order to produce a continuous set of hourly meteorological forcing data for each site for the period of interest (May through September 2012), the following data gap filling rules were applied following Rosolem et al. (2010):

1. if the gap was less than 3 h, it was filled by linear interpolation;

2. if the gap was greater than 3 h, the missing hours were replaced by values for the same hours averaged over the previous and subsequent 15 days;

3. if any additional gap filling was needed, the missing data were replaced by the average value for the specific hour calculated in the monthly mean diurnal cycle.

2.2 Noah Land Surface model

The Noah model, used operationally at the National Centers for Environmental Prediction (NCEP) for coupled weather and climate modeling (Ek, 2003), was adopted in this study. This LSM is also used in the NASA land information system (LIS) (Kumar et al., 2008), and in the Global (Rodell et al., 2004) and North American (Mitchell, 2004) Land Data Assimilation Systems (GLDAS and NLDAS, respectively).

The model contains four soil layers that extend two meters below the surface; specifically, a 10 cm thick surface layer, a 30 cm thick root-zone layer, a 60 cm thick deep root-zone layer, and a 1 m thick deep layer. The present study focuses on the first three layers of the model, where roots are prescribed to be present (0 to 1 m total depth). Soil-moisture parameterization is based on the one-dimensional Richards equation (Chen et al., 1996; Ek, 2003). Soil and vegetation parameters were defined from look-up tables and the Noah simulation run at hourly time steps at each selected site. A full description of Noah can be found in Chen and Dudhia (2001) and in Ek (2003), and the model is available from the Research Applications Laboratory at the Na-

tional Center for Atmospheric Research (RAL/NCAR) at http://www.ral.ucar.edu/research/land/technology/lsm.php.

2.3 Cosmic-ray Soil Moisture Interaction Code (COSMIC)

In this study, the COsmic-ray Soil-Moisture Interaction Code (Shuttleworth et al., 2013) is the forward observational operator used in data assimilation. COSMIC is characterized by a simple, physically based parameterization of belowground processes relevant for soil moisture estimates using cosmic-ray sensors, which includes (1) the degradation of the incoming high-energy neutron flux with soil depth, (2) the production of fast neutrons at a given depth in the soil, and (3) the loss of the resulting fast neutrons before they reach the soil surface. Despite its simplicity, COSMIC is robust and much more efficient than the traditional Monte Carlo neutron particle model commonly employed in cosmic-ray soil moisture applications (Franz et al., 2012b, 2013b; Rosolem et al., 2013). Here, the COSMIC is used to convert soil moisture profiles derived from the Noah into an equivalent neutron intensity, as seen by a cosmic-ray sensor. The code has been developed as part of the COSMOS network and is available at http://cosmos.hwr.arizona.edu/Software/cosmic.html.

2.4 Ensemble data assimilation

Data assimilation combines the information from observations and model predictions in order to estimate the state of a physical system, while recognizing both have some degree of uncertainty. Given the complexity of geophysical models in general, ensemble data assimilation techniques were originally developed to decrease the computational cost of the nonlinear filtering problem patterned after the Kalman filter (Kalman, 1960; Kalman and Bucy, 1961) by using a sample of model-state vectors to compute their statistical moments (i.e., mean and covariance) (Evensen, 1994, 2003; Houtekamer and Mitchell, 1998). In the hydrometeorological community, interest in ensemble data assimilation methods is growing rapidly for flood forecasting (Clark et al., 2008) and
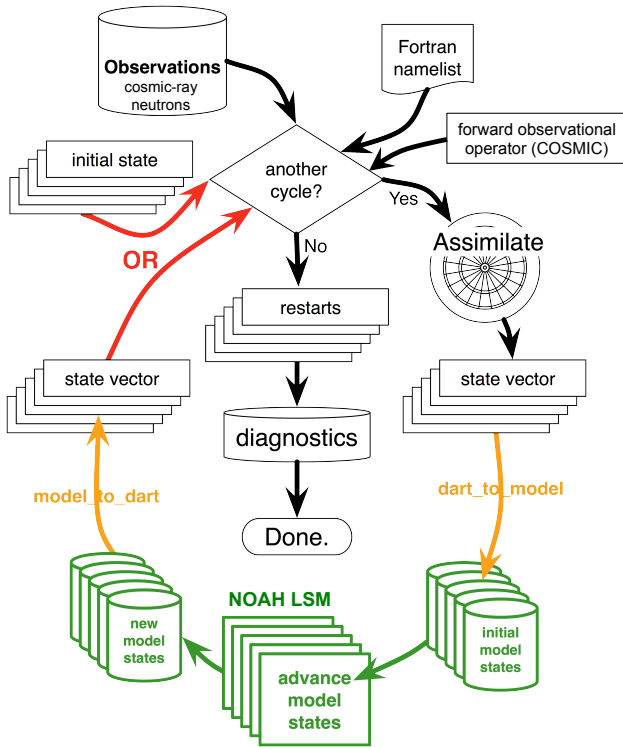
Figure 2. Schematic representation of the data assimilation and state update procedures in the Data Assimilation Research Testbed (DART) used in this study. Adapted from original DART diagram available at http://www.image.ucar.edu/DAReS/DART.

soil moisture applications (e.g., Draper et al., 2012; Kumar et al., 2012; Li et al., 2012).

The ensemble data assimilation method used in this study is an approximation of a general filtering algorithm developed using Bayes' theorem (Wikle and Berliner, 2007), and the method is described in detail by Anderson (2003, 2009). The probability distribution of a model state is approximated by an N-member sample of M-dimensional state vectors ($\boldsymbol{x}_i$; $i = 1, 2, \ldots, N$), where N is the ensemble size (in this study, $N = 40$) and each $\boldsymbol{x}_i$ is an M vector (e.g., soil moisture at each model layer). Because the error distributions for observations taken at different times are usually assumed independent in geophysical applications, each available observation can be assimilated sequentially. Hence, for simplicity, the assimilation of a single scalar observation, y, is used here. Bayes' theorem is as follows:

$$p(x|\mathbf{Y}, y) = p(y|x)\,p(x|\mathbf{Y})/\eta, \tag{1}$$

where x is the model state variable, $\mathbf{Y}$ is the set of all observations that have already been assimilated, which does not include the new observation, y, available at the current time, and η refers to a normalization factor. The ensemble assimilation procedure is summarized below.

1. Each ensemble member is advanced from the time of the most recently used observation to a time sufficiently close to the time of the next available observation using the Noah.

2. A prior ensemble estimate of y is created by applying the forward operator h (in this case, COSMIC) to each sample of the prior state.

3. An updated ensemble estimate of y conditioned on the new observation is computed from the prior ensemble estimate of y and the observed value, y_o, using Eq. (1). In this study, the Ensemble Adjustment Kalman Filter (EAKF) (Anderson, 2001) is used.

   In order to account for uncertainty in the model, the prior ensemble estimate of y is approximated as Normal$(\overline{y_p}, \sigma_p^2)$, where $\overline{y_p}$ and σ_p^2 are the sample mean and variance computed from the model ensemble, while the uncertainty in the observation, y_o, is defined as σ_o^2. Given the nature of the cosmic-ray sensor and the large number of counts per integration time (i.e., hourly), the assumption of observation uncertainty to be normally distributed (with $\sigma_o^2 = y_o$) is appropriate. The product of Normal$(\overline{y_p}, \sigma_p^2)$ and Normal(y_o, σ_o^2) in Eq. (1) is computed resulting in a Gaussian updated distribution for y, Normal$(\overline{y_u}, \sigma_u^2)$ with an updated variance (σ_u^2) and mean ($\overline{y_u}$), defined as:

$$\sigma_u^2 = \left[\left(\sigma_p^2\right)^{-1} + \left(\sigma_o^2\right)^{-1} \right]^{-1} \tag{2}$$

and

$$\overline{y_u} = \sigma_u^2 \left[\left(\sigma_p^2\right)^{-1} \overline{y_p} + \left(\sigma_o^2\right)^{-1} y_o \right], \tag{3}$$

respectively. In the EAKF, the prior ensemble distribution of y is then shifted and linearly contracted to create an updated ensemble with sample statistics as in Eqs. (2) and (3). Observation increments are computed as:

$$\Delta y_i = \sqrt{\sigma_u^2/\sigma_p^2}\left(y_{p,i} - \overline{y_p}\right) + \overline{y_u} - y_{p,i};$$
$$i = 1, 2, \ldots, N, \tag{4}$$

where the subscript i refers to ensemble member.

4. Increments to the prior ensemble of each state-vector element ($x_{j,i}$, where j refers to an element of the state vector, while i refers to an ensemble member) are computed by linearly regressing the observation increments (Δy_i) onto each state-vector component independently using the prior joint sample statistics, so that

$$\Delta x_{j,i} = \left(\sigma_{p,j}/\sigma_p^2\right)\Delta y_i \; ; \; j = 1, 2, \ldots, M;$$
$$i = 1, 2, \ldots, N. \tag{5}$$

Table 2. Perturbation magnitudes of meteorological inputs used by Noah for individual ensemble members in this study. The perturbation distribution is either Lognormal (i.e., multiplying the reference variable) or Normal (i.e., adding to or subtracting from a reference value). Values within parentheses correspond respectively to mean and standard deviation. Notice, vegetation greenness fraction has been added to the list given its strong sensitivity in Noah (Miller et al., 2006). The adopted magnitude values follow standard procedures described in the literature, including Dunne and Entekhabi (2005), Kumar et al. (2012), Margulis et al. (2002), Reichle and Koster (2004), Reichle et al. (2008, 2007, 2002), Sabater et al. (2007), Walker and Houser (2004), Zhang et al. (2010), and Zhou et al. (2006).

Noah forcing	Perturbation magnitude
Wind speed ($m\,s^{-1}$)	Lognormal(1,0.3)
Air temperature (K)	Normal (0,5)
Relative humidity (fraction)	Lognormal (1,0.2)
Surface pressure (Pa)	Normal (0,10)
Incoming shortwave radiation ($W\,m^{-2}$)	Lognormal (1,0.3)
Incoming long-wave radiation ($W\,m^{-2}$)	Normal (0,50)
Precipitation rate ($kg\,m^{-2}\,s^{-1}$)	Lognormal(1,0.5)
Vegetation greenness fraction (-)	Normal(0,0.05)

The Noah, the COSMIC operator and COSMOS observations have all been implemented into the Data Assimilation Research Testbed (DART) framework (Anderson et al., 2009). Figure 2 shows a schematic diagram of the assimilation and state update procedures used in this study. DART is an open-source community facility that provides software tools for ensemble data assimilation research in geosciences. The modularity of DART makes the interface to new models and observations straightforward and clean. The DART code is available at http://www.image.ucar.edu/DAReS/DART.

3 Experimental setup

3.1 Perturbed meteorological forcing and initial conditions

In order to ensure that appropriate ensemble spread throughout the assimilation procedure, time series of cross-correlated perturbation fields were generated for all meteorological forcing inputs from Noah and applied to each individual ensemble member (a total of 40 members), similar to the approach used by Shuttleworth et al. (2013); see Table 2 for more details. In all cases, the Latin Hypercube random sampling method (McKay et al., 1979) was used to generate uniformly distributed soil moisture values (for each model layer), varying between minimum and saturated soil water contents in the model. We therefore assume no information about the soil moisture profiles prior to the initial simulation time step (i.e., 1 May 2012). All remaining model states
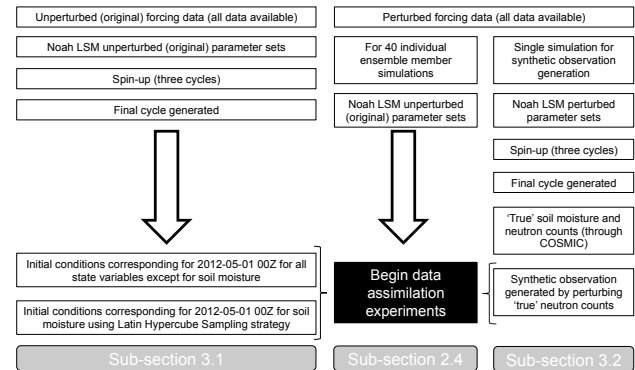

Figure 3. Experimental setup used in this study for data assimilation of synthetic observations of cosmic-ray neutrons.

were obtained from the previous time step (30 April 2012 at 23:00 UTC) from a spin-up simulation with four repeated cycles (spin-up periods shown in Table 1) using the original meteorological forcing data (i.e., unperturbed) and original model parameters (Fig. 3).

3.2 Synthetic observations

We employ the use of synthetic observations in this study in order to better assess the advantages and limitations of this novel cosmic-ray technology. The approach allows a direct comparison between simulated and "true" soil moisture states at the three sites at which no additional soil moisture observations are available at the same spatial scale measured by the cosmic-ray sensors. The use of synthetic observations in data assimilation studies targeted at satellite remote-sensing soil moisture missions continues to show great importance for advancing our understanding of regional hydrometeorological modeling (Kumar et al., 2012; Nearing et al., 2012; Reichle et al., 2008).

For each studied location, synthetic neutron intensity observations (referred to in the rest of the article simply as "observations") are generated directly from the Noah in combination with the COSMIC. An additional set of perturbed meteorological forcing (not from the original pool of ensemble members) is generated following the same procedure described in the previous section. Additionally, 10 parameters, originally identified as influential using a simple "one-at-a-time" sensitivity analysis approach (not shown), are perturbed within a ±10 % range from their default values to generate a single parameter set (for each location) used in Noah for the synthetic output generation in a "nearly-identical twin experiment". The idea is to emulate some unexpected (or unidentifiable) variability observed in soil moisture due to small spatial-scale heterogeneities (Crow et al., 2012; Famiglietti et al., 2008; Western and Blöschl, 1999) through changes in key parameter values in the Noah model. Identified parameters include *fxexp* (bare soil evaporation

exponent), *refdk* (reference value for saturated hydraulic conductivity), *refkdt* (reference value for surface infiltration parameter), *bb* (Clapp and Hornberger "b" parameter), *refsmc* (soil moisture threshold for onset of some transpiration stress), *drysmc* (top-layer soil moisture threshold at which direct evaporation from soil ceases), *wltsmc* (soil moisture wilting point), *satdk* (saturated hydraulic conductivity), *satdw* (saturated soil diffusivity), and *rs* (minimum stomatal resistance). Soil porosity was not included and hence the default values were used for each site. We use the coefficient of variation from the in situ dry-soil bulk density collected within the cosmic-ray footprint at all three sites combined as a proxy for the perturbation magnitude (i.e., ±10 %) applied to parameter variations to account for uncertainty due to spatial heterogeneity embedded in the single-point simulation (please refer to the Table S1 in the Supplement for detailed description of Noah parameter values). Such perturbations applied both to the meteorological forcing and to above-mentioned parameters produce slightly different soil moisture dynamics (and hence "true" neutron counts) when compared to COSMIC-derived neutron counts when forced with Noah with the original parameter set (not shown). For each site, the spin-up corresponds to the period shown in Table 1, repeated four times (i.e., four cycles).

After the spin-up period, the simulated soil moisture at each soil layer from May through September 2012 was then used as input data for the COSMIC to generate a "true" equivalent neutron intensity time series (counts per hour). This "true" neutron intensity is finally perturbed following a probability distribution associated with the uncertainty observed in the actual cosmic-ray sensors, as described by Zreda et al. (2008) ($\sigma^2_{N_{counts}} = N_{counts}$; where N_{counts} is the neutron intensity), and a time series of hourly synthetic observations is produced for each site. In addition, a subset from the hourly time series is produced assuming observations are available every other day (for simplicity, defined always at noon GMT). The 2-day frequency was selected because it is similar to the temporal resolution likely to be achieved by the most recent satellite remote-sensing soil moisture missions (Brown et al., 2013; Entekhabi et al., 2010; Kerr et al., 2010). In order to avoid undesired instabilities at the beginning of the simulation, no observation is assimilated during the first 24 h. A schematic diagram of the experimental setup is shown in Fig. 3.

We use these observations in our experiments to evaluate the ability of Noah to reproduce the synthetically observed neutron intensity, and consequently to analyze the updated soil moisture profile against the "true" soil moisture state. Notice that the neutron intensity time series produced in this study are not rescaled to correspond to the location of the original COSMOS probe site in the San Pedro, as discussed by Zreda et al. (2012). This is because we want to preserve the site-specific count statistics to better describe measurement uncertainty (lower count rates, on average, will tend to be more uncertain compared to locations at which count rates

are relatively high). Moreover, there are no systematic biases between observed and simulated neutron counts (not shown), and data assimilation is performed with zero-mean random errors only (Dee, 2005). Observing System Simulation Experiments (OSSEs), such as those proposed in this study, allow us to accurately isolate the signal in the neutron measurements that comes directly from the soil moisture (through the COSMIC) for more rigorous analyses. Model structural deficiencies, which could potentially result in systematic biases, are therefore not accounted for, and observation uncertainties not related to soil moisture (e.g., atmospheric water vapor, changes in biomass) do not impact the simulations. In addition, independent observations of soil moisture profiles representing similar horizontal effective measurement areas are generally not available.

4 Results

4.1 Assimilation of neutron counts

For all analyzed sites, the assimilation of summertime neutron observations in Noah improves the dynamics relative to the true neutron count time series in comparison with the no data assimilation case (i.e., "no DA") (Fig. 4). The ensemble mean of the prior distribution is used for all ensemble simulations throughout this study. As discussed in Section 1, the higher the neutron counts at a specific location, the lower the integrated soil moisture is expected to be. Rainfall events are therefore associated with sharp decreases in the neutron counts followed by a relatively slower dry-down period. Noticeably, the Kendall site (Fig. 4a) is characterized by an initial long period with very low or no rain (pre-monsoon) until early July, followed by more frequent rainfall events (monsoon) between July and early September. Both the Nebraska and Park Falls sites (Fig. 4b and c, respectively) show the opposite rainfall pattern with an initial period with frequent rainfall (slightly more frequent at Park Falls) until about mid-June–early July, followed by a relatively dry period for about 1–2 months (slightly longer at Park Falls). Notice that 2012 was one of the driest years on record for the Midwestern USA (Blunden and Arndt, 2013).

Both assimilation cases (i.e., with hourly available observations – "DA 1-hour" shown as the red line, with observations available once every 2 days, and "DA 2-day" shown as green circles) suggest superior performance compared with the case without assimilation (blue line; Table 3). Overall, the DA 1-hour case approaches more rapidly to the true neutron counts and also exhibits a tendency for relatively smaller differences when compared to the DA 2-day case. Notably, at the onset of the monsoon at Kendall (i.e., early July), the low-frequency assimilation case neither reproduces the high-frequency dynamics nor the DA 1-hour case (Fig. 4a). At the Nebraska and Park Falls sites (Fig. 4b and c), there is not much improvement in Noah-derived neutron counts from the
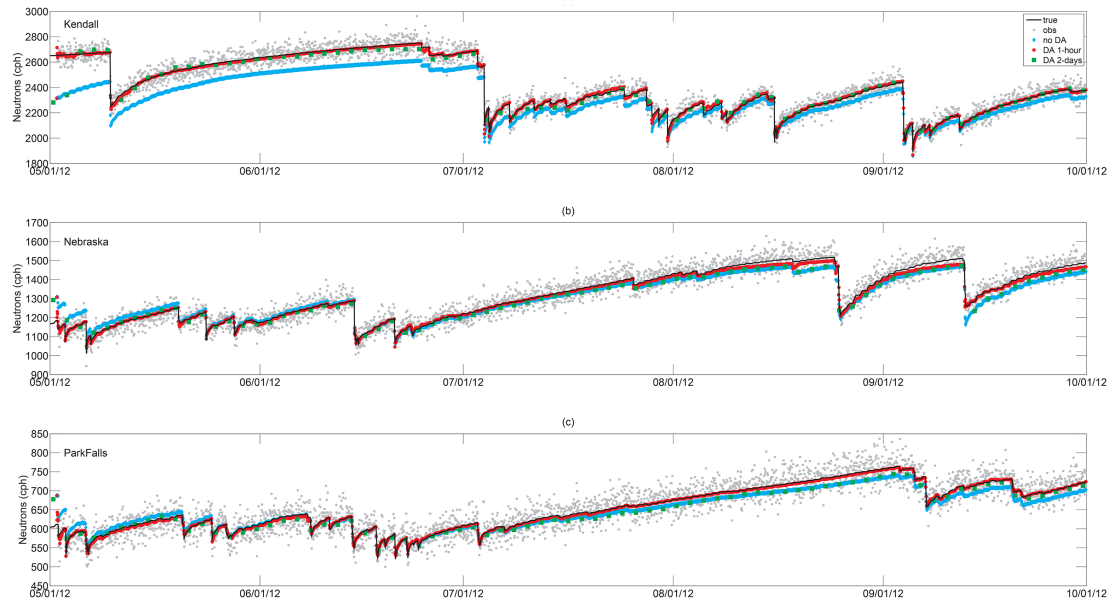
Figure 4. Equivalent neutron intensity (counts per hour – cph) simulated by Noah coupled to COSMIC without (no DA) and with data assimilation characterized by low- and high-frequency retrievals (respectively, DA 2-day and DA 1-hour) compared to synthetic observations (obs) and true intensities. The ensemble mean of the prior distribution is shown for all ensemble simulations.

Table 3. Summary of statistics computed for Noah for assimilation of synthetic neutron intensity measurements in counts per hour (cph). Metrics are computed with respect to both true counts and synthetic observations, respectively "w.r.t. True" and "w.r.t. Obs". The ensemble mean of the prior distribution is used for all ensemble simulations.

Site	Simulation	Mean bias		RMSE		Total spread	R^2	
		w.r.t. Obs	w.r.t. True	w.r.t. Obs	w.r.t. True		w.r.t. Obs	w.r.t. True
Kendall	no DA	−89	−90	119	109	96	0.89	0.94
	DA 2-day	−9	−13	63	60	57	0.91	0.92
	DA 1-hour	0	−1	63	60	50	0.91	0.92
Nebraska	no DA	−15	−14	49	32	51	0.90	0.97
	DA 2-day	−13	−15	45	28	40	0.89	0.97
	DA 1-hour	−8	−8	38	12	37	0.93	1.00
Park Falls	no DA	−8	−8	30	15	36	0.82	0.98
	DA 2-day	−6	−8	27	14	27	0.81	0.96
	DA 1-hour	−2	−2	25	3	26	0.84	1.00

DA 2-day relative to the no DA in periods where little or no rainfall occurs.

The use of synthetic observations ensures that the neutron signal from the measurement solely comes from direct contribution of soil moisture dynamics, and that any model structural deficiency does not impact the results. Hence, a potential limitation of an OSSE is that the results can be very optimistic in comparison to a data assimilation experiment using real observations. For instance, when comparing against real observations, one would like the RMSE (which represents the accuracy of the ensemble mean state relative to the observations) to be comparable to the total spread (which contains both the ensemble spread and observational error signals). In

that case, the RMSE is defined as the square root of the average squared difference between the model estimates and the observations, while the total spread is defined as $\sqrt{\sigma_p^2 + \sigma_o^2}$, where $\left(\sigma_p^2 + \sigma_o^2\right)$ represents the total variance (i.e., the sum of the ensemble variance, σ_p^2, plus the observational error variance, σ_o^2). In our case, however, one way to test the success of an OSSE is to compare the RMSE computed with respect to the "true" observations with the ensemble spread (σ_p) directly because the variance of the "true" observations (σ_o^2) is, by definition, zero.
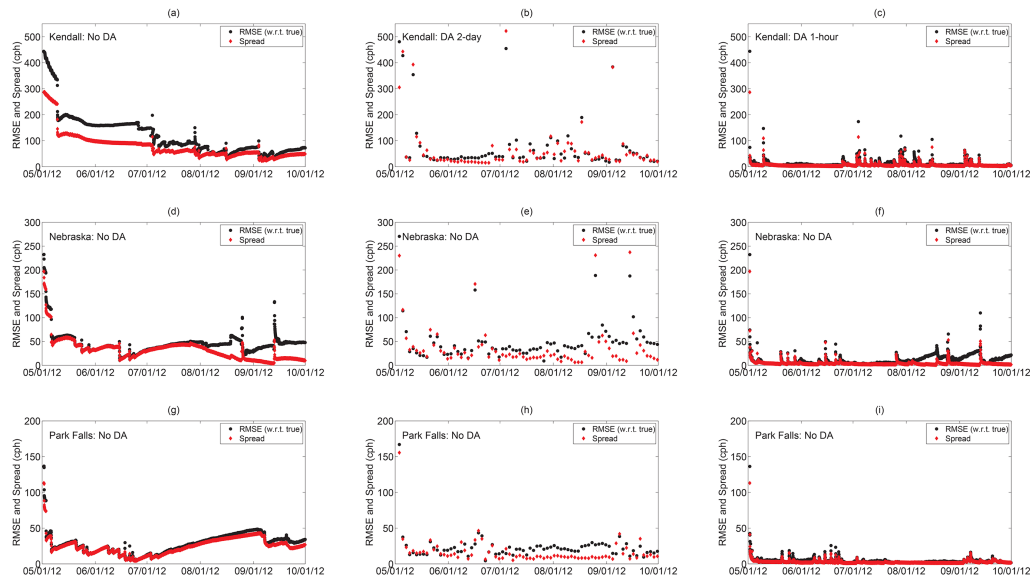
Figure 5. Root-Mean-Squared Error (RMSE) calculated for the ensemble mean relative to the "true" observations (black circles) in comparison to the ensemble spread (red diamonds). The ensemble mean of the prior distribution is used for all ensemble simulations.

Figure 5 shows the comparison between the RMSE (black circles) and spread (red diamonds) for all analyzed cases at all sites. Overall, the magnitudes for the spread compare well with those for RMSE, suggesting that this is a successful assimilation experiment. Notice that these two quantities tend to be closest to each other for the DA 1-hour case (right column), and the largest differences are seen for the no DA case (left column). The rapid reduction in total spread at the Kendall site with time for the no DA case is due to the fact that soil moisture presents a strong "damping" signal, especially in the first few months when little rainfall occurs (May–July). This is fundamentally the same behavior observed when models are "spun up" or "warmed up" for a selected period of time prior to their final analysis simulation. Consequently, individual ensemble members move towards a preferred state. Notice that this behavior is not clearly observed at the Nebraska and Park Falls site, at which rainfall occurs continuously in the first months (May–July). In comparison to the no DA case, RMSE for both assimilation cases are reduced, with the lowest RMSE values found for the DA 1-hour case.

As expected, the time at which rainfall occurs appears to control the characteristics of both statistical quantities. We therefore identified two patterns that emerged in Fig. 5. The first pattern is associated with a rapid increase in both RMSE and spread during large rainfall events (rapid reduction in neutron counts, as shown in Fig. 4). These are more clearly observed for the DA 2-day cases (middle-column) at Kendall (mid-May, early July, mid-August, and early September) and at Nebraska (mid-July, late August, and mid-September). These peaks are substantially reduced when observations of neutron counts are assimilated at higher frequency (i.e., DA

1-hour, as shown in the right column). No large rainfall event was identified at the Park Falls site (Fig. 4). Consequently, this pattern was not observed in Fig. 5.

The second pattern relates to the overall timing of the summer rainfall. At the Kendall site, once the monsoon period begins (early July), the assimilation of observations successfully constrains the model, which produces consistent equivalent neutron counts (Fig. 5b and c). In other words, rainfall pulses provide "new information" to the assimilation system. For the two other sites (Nebraska and Park Falls), an active rainfall period lasts until early July and is then followed by a period of low or no rainfall (arguably, no substantial "information" to the assimilation system). In this case, we observe a tendency for lower spread values in comparison to RMSE at both sites for the DA 2-day case. This tendency disappears when high-frequency observations are assimilated (i.e., DA 1-hour) at the Park Falls site. For the Nebraska site, although still present, the tendency is reduced for the DA 1-hour. These results highlight the quality of the OSSEs carried out in this study, as well as the distinct performance of the assimilation system due to different timing in rainfall events occurring at all three AmeriFlux sites.

Finally, the results summarized in Table 3 show better overall performance for DA 1-hour compared to DA 2-day, with both cases being almost always superior to the no DA case. In almost all cases, computed statistics with respect to the true counts are better than those computed with the synthetic observations. This is expected because an additional degree of randomness is introduced in the synthetic observations (i.e., light-gray circles in Fig. 4). The degree of improvement compares well with the results from Shuttleworth et al. (2013).
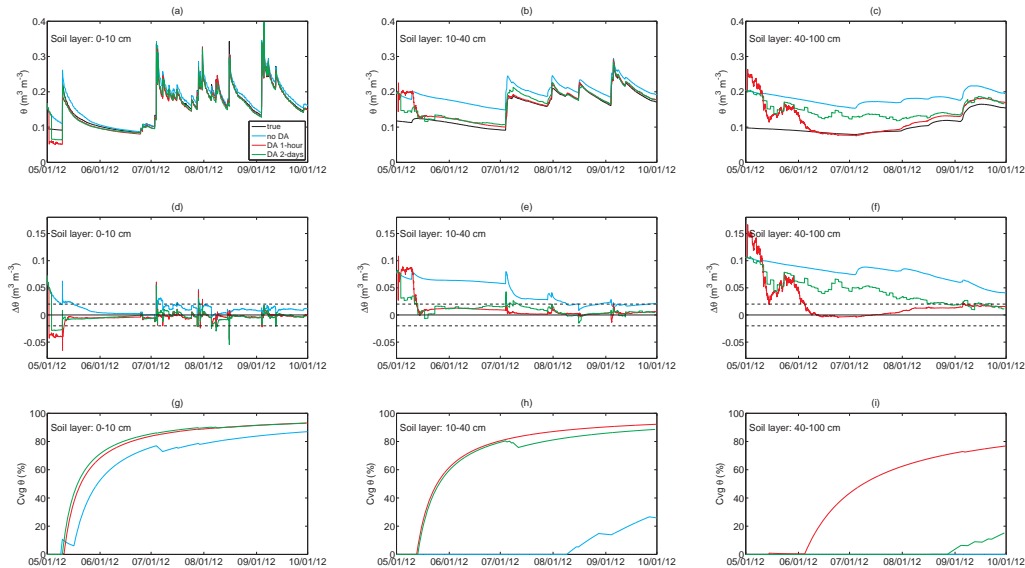
Figure 6. Comparison of soil moisture dynamics at the Kendall site for the first three soil layers in Noah. Top row: simulated soil moisture (θ) without (no DA) and with data assimilation, characterized by low- and high-frequency retrievals (respectively, DA 2-day and DA 1-hour) compared to the true soil moisture states. Middle row: the difference between simulated soil moisture and the true states ($\Delta\theta$) within pre-defined uncertainty ranges (dashed black lines). Bottom row: convergence criterion within uncertainty ranges. Results show actual model time steps (i.e., hourly). The ensemble mean of the prior distribution is shown for all ensemble simulations.

Table 4. Summary of statistics computed for Noah for assimilation of synthetic neutron intensity measurements for all sites. All metrics are calculated only when individual layer convergence is above 40 % for the case DA 1-hour (see bottom panel of Figs. 6, 7, and 8), and with respect to the true soil moisture state. The ensemble mean of the prior distribution is used for all ensemble simulations. Numerical values are rounded to the first three decimal points.

Noah soil moisture ($m^3\,m^{-3}$)	Mean bias			RMSE			Spread			R^2		
	No DA	DA 2-day	DA 1-hour	No DA	DA 2-day	DA 1-hour	No DA	DA 2-day	DA 1-hour	No DA	DA 2-day	DA 1-hour
Kendall												
θ_1 (0–10 cm)	0.009	−0.003	−0.003	0.011	0.006	0.005	0.019	0.007	0.003	0.988	0.990	1.000
θ_2 (10–40 cm)	0.037	0.009	0.006	0.042	0.011	0.007	0.033	0.012	0.006	0.907	0.981	0.995
θ_3 (40–100 cm)	0.071	0.030	0.009	0.072	0.033	0.012	0.051	0.032	0.015	0.906	0.872	0.989
Nebraska												
θ_1 (0–10 cm)	0.004	0.005	0.001	0.010	0.009	0.004	0.016	0.008	0.003	0.978	0.987	0.996
θ_2 (10–40 cm)	0.007	0.011	0.006	0.017	0.013	0.007	0.022	0.009	0.003	0.962	0.987	0.998
θ_3 (40–100 cm)	0.012	0.012	0.009	0.012	0.012	0.009	0.038	0.018	0.007	0.999	0.998	0.993
Park Falls												
θ_1 (0–10 cm)	0.005	0.007	0.001	0.009	0.009	0.003	0.018	0.008	0.003	0.984	0.985	0.996
θ_2 (10–40 cm)	0.006	0.008	0.002	0.010	0.010	0.004	0.022	0.009	0.003	0.986	0.987	0.997
θ_3 (40–100 cm)	0.007	0.013	0.005	0.011	0.015	0.007	0.031	0.013	0.005	0.974	0.980	0.990

4.2 Impact of near-surface cosmic-ray neutrons on simulated soil moisture profiles

In the case of cosmic-ray sensors, the dynamics of equivalent neutron counts observed can be assumed to be a proxy for integrated, depth-weighted variation of soil moisture at sub-kilometer scales, as shown by Shuttleworth et al. (2013). Here, we expand this analysis by assessing how well all root-zone layers in the Noah (prescribed as the first 1 m of soil in the model) are simulated with and without the assimilation

of observed neutron counts. The effective sensor depth computed from the synthetic observations at all three sites varies on average from ∼ 12 cm during the wet period to ∼ 20 cm in the dry months. This corresponds to the entire surface (first) soil layer of Noah with an additional contribution from the second soil layer in the model (10–40 cm layer). Overall results are summarized in Table 4 and presented for each site in Figs. 6, 7, and 8.

In those figures, the left column is related to the first soil layer, and the right column is related to the deepest layer
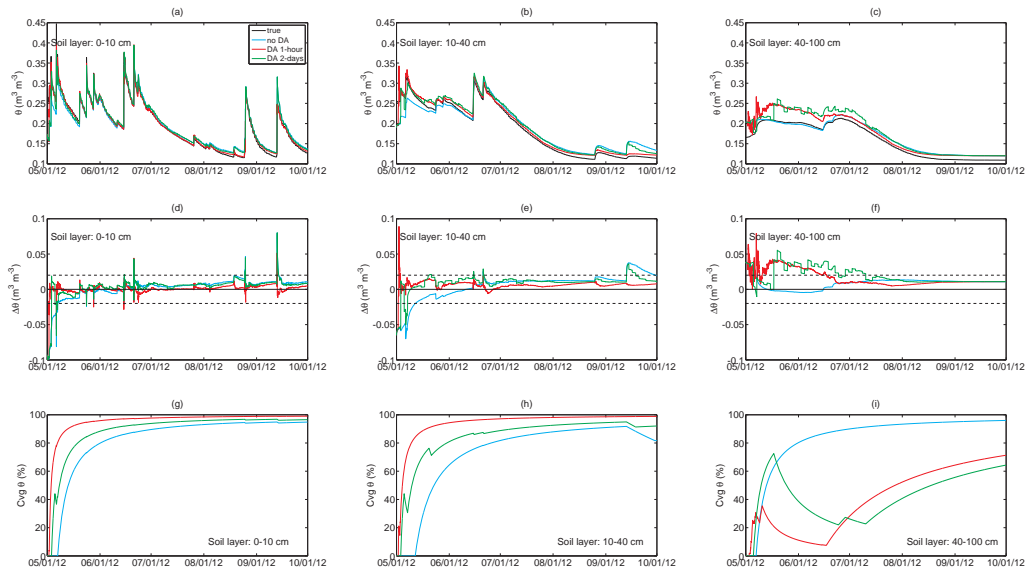
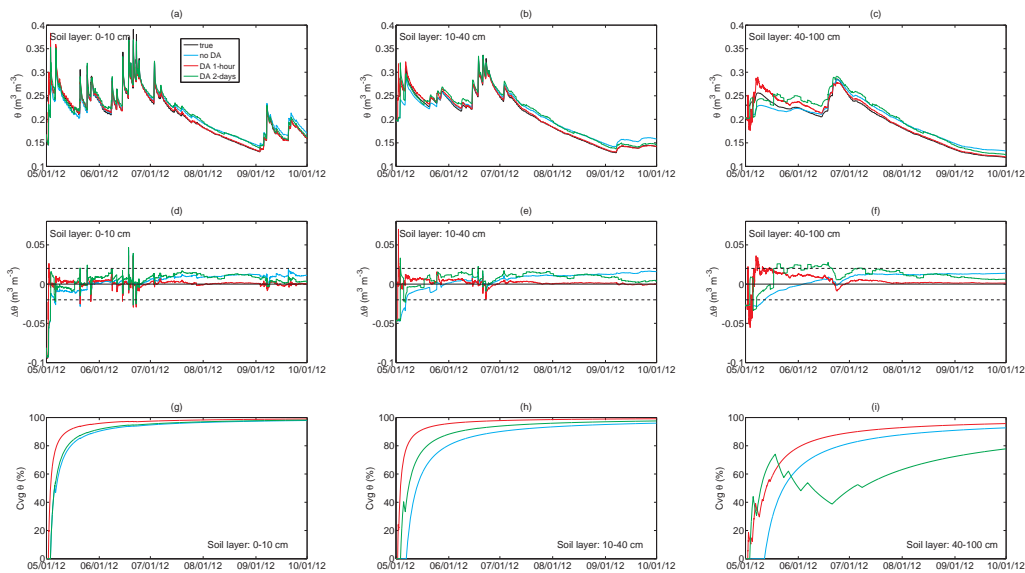**Figure 7.** Same as Fig. 6 but for Nebraska.

Figure 8. Same as Fig. 6, but for Park Falls.

analyzed. The top row corresponds to the actual soil moisture simulated by Noah for the three cases (i.e., no DA, DA 2-day, and DA 1-hour) in comparison to the true soil moisture state (same color-coding as before). The middle row shows the difference between the Noah-derived and true soil moisture. We selected an "uncertainty range" of $\pm 0.02\,\mathrm{m^3\,m^{-3}}$ as our target for comparison, which is similar to the accuracy found in more traditional point-scale measurements (Topp et al., 1980) and also comparable to the accuracy of cosmic-ray sensors (Franz et al., 2012a; Rosolem et al., 2013). Note that the target accuracy from satellite remote-sensing products is twice as big, as discussed by Brown et al. (2013), Entekhabi

et al. (2010), and Kerr et al. (2010). The bottom row corresponds to a simple convergence criterion based on the results from the middle row. For each hourly time step, we check whether the difference with respect to the true soil moisture is within the "uncertainty range". If it is within this range, the value is added to the current number of counts, and the percentage convergence is taken with respect to the total number of points analyzed at that given time. As an example, if the first point found within the "uncertainty range" is located in position 50 of the time array, its convergence is computed as 2 % (i.e., 1/50). If the next time step is also within this range, its convergence is computed as ~ 3.9 % (i.e., 2/51), and so

on. With this simple metric, we can not only determine the overall percentage of hours when the difference was within this uncertainty range (obtained at the end of the simulation), but also how the convergence evolves as the simulation period progresses.

At the Kendall site, the results suggest overall improved performance of Noah for all soil layers (including those beyond the sensor effective depth) when observed neutron counts are assimilated, regardless of the availability of observations (Fig. 6a–f). Differences between DA 1-hour and DA 2-day cases are larger at deeper soil layers, with DA 1-hour showing superior performance. For the no DA case, only the soil moisture at the first layer in the model is within the uncertainty range for the majority of the simulated period. The soil moisture for the DA 2-day case compares relatively well with the true soil moisture at the first two layers, but estimated soil moisture in the third layer is almost always outside of the uncertainty range. The DA 1-hour case, however, shows a remarkable response to neutron count and effectively simulates the soil moisture dynamics at all Noah soil layers (basic statistics are calculated and presented in Table 4).

The convergence calculated for the Kendall site suggests that, overall, soil moisture is constrained more effectively when observations of cosmic-ray neutrons are assimilated into Noah (Fig. 6g–i). For the first soil layer, total convergence levels are high in all cases and little difference is observed between the two DA cases. The benefit of assimilating observed neutron counts is more clear in the results for the second layer, with no substantial differences between the high- and low-frequency assimilation strategies. However, the impact of higher-retrieval frequency becomes evident in the third soil layer in which soil moisture is only successfully constrained in the DA 1-hour case.

The results from the Nebraska and Park Falls sites are comparable and they show superior performance of Noah when assimilating neutron counts at high-frequency (Figs. 7a–f and 8a–f). Surprisingly, for the first two soil layers in Noah, the dynamics of soil moisture obtained from the ensemble average for DA 2-day is similar to the model behavior for the no DA case. In addition, no DA soil moisture at the deepest analyzed layer at the Nebraska site follows the true soil moisture states quite well. This is likely related to the fact that the initial conditions randomly obtained in the model were already similar to the true soil moisture state (in terms of ensemble averages) for the no DA case, although the overall magnitude of the spread is much larger compared to assimilation cases (Table 4). At Park Falls, the results from the deepest soil layer analyzed show superior performance of DA 1-hour while no DA and DA 2-day have similar dynamics, especially after late June.

The convergence criterion computed for the first two soil layers in Noah at the Nebraska and Park Falls sites (Figs. 7g–h and 8g–h) are slightly different from the results discussed for the Kendall site (Fig. 6g–h). First, the percentage of points within the uncertainty range at these two sites is greater than the percentage values obtained at Kendall (compare, for instance, the DA 1-hour case across all sites). There is a much sharper increase in the convergence criterion with time at these two sites, as opposed to the pattern observed for Kendall. However, unlike the Kendall site, where the patterns of both DA cases were somewhat similar, it is much clearer for both the Nebraska and Park Falls cases that the DA 1-hour is able to update soil moisture much more rapidly than the DA 2-day when compared to the response to the no DA case. As mentioned previously, the convergence results for the no DA case at the third soil layer in the model are likely to be related to the initial conditions from the ensemble mean being already too close to the true states (Figs. 6i and 7i).

4.3 Impact of retrieval frequency on simulated soil moisture dynamics

The previous sub-section reports the improved ability of Noah to estimate soil moisture profiles when assimilating cosmic-ray neutron counts measured aboveground, and included some initial comparison between assimilation frequencies (DA 1-hour and DA 2-day). In this section, we compare the "average" performance of Noah for continuous periods of 2 days after the cosmic-ray neutron measurement is assimilated into the model throughout the simulation period. The aim is to evaluate the Noah performance within individual time windows when neutron measurements are assimilated every 2 days, every hour, or not assimilated at all. In this study, the RMSE of soil moisture is calculated with respect to the true state for a fixed time window of 2 days applied throughout the entire simulation period. For comparison, the results discussed in the previous section were based on actual model simulations at hourly timescales. The results are presented in Fig. 9 with top, middle, and bottom rows, corresponding respectively to the Kendall, Nebraska, and Park Falls sites, with left and right columns corresponding to the shallowest and deepest Noah soil layers analyzed in this study (same color coding as shown in previous figures).

The first noticeable result from Fig. 9 is that the average performance of Noah (i.e., using the 2-day time windows) when trying to simulate true soil moisture profiles is best when neutron measurements are assimilated at hourly timescales (i.e., DA 1-hour) at all sites. At the Kendall site, which is characterized by a long dry period followed by the monsoon onset early in July, the performance of Noah for the DA 2-day case is similar to that obtained with DA 1-hour at the first two layers of the model (Fig. 9a–b), and slightly worse at the deepest layer (Fig. 9c). Surprisingly, a different pattern emerges from both the Nebraska and Park Falls sites at which an initial period of frequent rainfall is followed by a relatively long dry period, which also starts in July (Fig. 9d–i). In those cases, the performance of DA 2-day is not improved substantially in comparison to no DA, and a noticeable increase in RMSE is observed in both cases right after rainfall ceases in July. Unlike the DA 1-hour case,
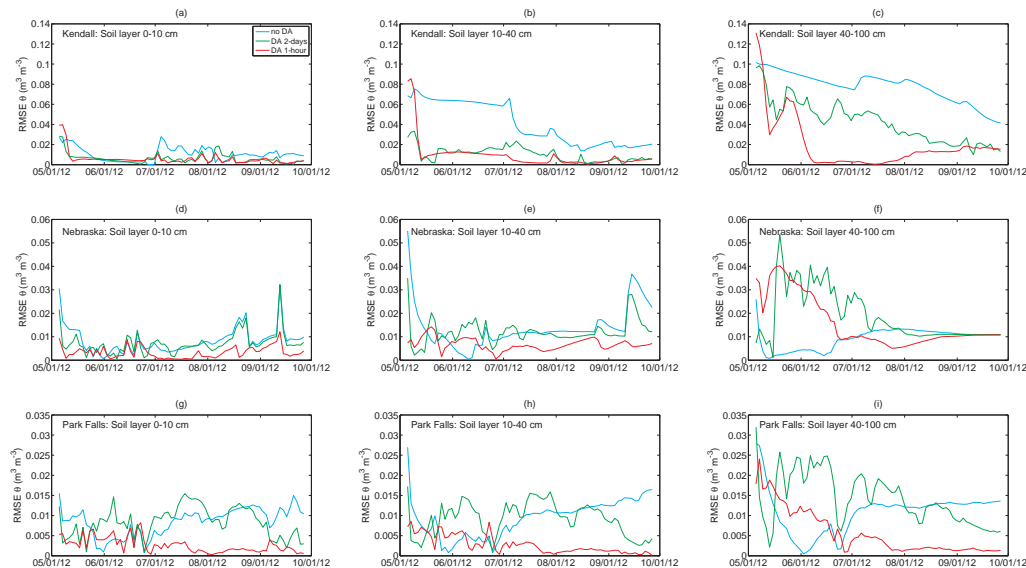
Figure 9. Comparison of Noah performance in representing soil moisture dynamics for the first three soil layers with respect to the true soil moisture state. The metric used is the Root-Mean-Squared Error (RMSE) calculated over individual 2-day periods continuously. Results are shown for Noah without (no DA) and with data assimilation, characterized by low- and high-frequency retrievals (respectively, DA 2-day and DA 1-hour). The ensemble mean of the prior distribution is used for all ensemble simulations.

the DA 2-day case allows for Noah to freely advance in time for the rest of the 2-day period once it has assimilated the neutron count measurement, and, because the true simulation was generated with a different set of parameters than the cases analyzed here, model simulations in the DA 2-day case are unable to represent the dynamics of dry-down appropriately due to different soil properties. The lack of rainfall, in this case, reduces the potential magnitude for soil moisture updates (i.e., "model innovation"), and hence the dynamics of the model are little improved. The results shown here suggest that the performance of summertime cosmic-ray neutron data assimilation may be slightly dependent on climatological conditions (i.e., meteorological forcing) and the period during which rainfall occurs in the summer. Moreover, it depends on model uncertainties due to lack of representativeness of key soil and vegetation properties at the scale of interest (here, accounted for by the fact that true soil moisture is generated from a model simulation obtained with slightly perturbed parameter values).

5   Summary and conclusions

The use of cosmic-ray neutron sensors for soil moisture monitoring has been fast growing because the technique provides root-zone soil moisture estimates at unprecedented spatial scales and at high temporal resolution. This paper evaluates the ability of a land surface model to translate the information obtained from cosmic-ray neutrons observed aboveground into soil moisture estimates for individual soil layers. A nearly-identical twin experiment approach is adopted in

which observations of cosmic-ray neutrons were generated from a land surface model with a slightly different configuration (perturbed key soil and vegetation parameters). Below, we discuss the implications and summarize the main findings of this work.

How effectively is the information from aboveground cosmic-ray neutrons translated to individual soil moisture layers in the model?

When assimilating neutron counts at high frequency, the performance of the land surface model is remarkably improved in comparison with the soil moisture profiles simulated without data assimilation. This finding is observed for all three biomes with a degree of improvement varying slightly from site to site. Of importance, we found that water in the soil is better estimated at depths well below the effective sensor depth and encompassing the entire rooting zone in the model. Therefore, the high observational frequency of the cosmic-ray sensors can potentially introduce additional benefits relative to assimilating local/regional soil moisture observations from satellite remote-sensing products available at coarser temporal resolution. However, care must be taken when accounting for measurement uncertainty by removing any potential signal in the measurement from other sources of hydrogen (atmospheric water vapor, water in biomass), hence isolating or maximizing the soil moisture information content in the measurement. Another important aspect is to ensure sufficient ensemble spread from the model to avoid, for instance, filter divergence (overconfidence in the model),

or, alternatively, directly inserting observations with little or no model influence (overconfidence in the observations) (Anderson, 2007; Hamill et al., 2001; Houtekamer and Mitchell, 1998).

How does frequency of available observations of cosmic-ray neutrons influence model performance?

We use the RMSE calculated for every 2-day time window as a metric for model performance. At the Kendall site, DA 1-hour and DA 2-day showed good agreement for soil moisture in the first two layers of the model (0–10 and 10–40 cm). However, the benefits of high-frequency retrievals in the case of cosmic-ray neutron observations is also observed for the third soil layer in Noah (40–100 cm), where DA 1-hour is much superior to DA 2-day. Particularly to the Noah, the distribution of roots is directly proportional to the thickness of each soil layer. Therefore, the third layer of the model plays a significant role in determining evapotranspiration rates at the surface. Summertime is characterized by an initial relatively dry period, which lasts for about 2 months, followed by the monsoon.

Unlike the results at Kendall, the comparison between DA 1-hour and DA 2-day for Nebraska and Park Falls suggest that the performance of Noah for the DA 1-hour case is always superior to that from DA 2-day in all soil layers analyzed. Surprisingly, the model performance for the DA 2-day case is not much different from simulations made without assimilating cosmic-ray neutron counts (i.e., no DA case). A distinct characteristic from both the Nebraska and Park Falls sites in comparison to Kendall is the overall dynamics of soil water in the summertime. At Nebraska and Park Falls, a relatively wet period with frequent rainfall is observed at the beginning of the summertime period, lasting for about 2 months, and followed by a relatively dry period with low or no rainfall. Overall, the benefits of assimilating neutron measurements at relatively higher frequency are more clearly observed at the Nebraska and Park Falls sites relative to the semi-arid Kendall. This could indicate that the assimilation performance of summertime cosmic-ray measurements at high temporal resolution may depend not only on heterogeneity of soil properties (accounted for by slightly perturbing model parameter from true soil moisture states), but also slightly on meteorological forcing and its climatology (namely, rainfall). Also, these findings suggest an important role of high-frequency measurements to better constrain soil moisture states simulated by hydrometeorological models when applied to drought monitoring, given that the summer of 2012 was one of the driest on record in the Midwestern USA region.

Due to the characteristics of the sensor, the integration time used to compute neutron intensity should potentially be longer than 1 h at some locations. In practice, this is done to reduce the uncertainty in the measurement and consequently ensure an accurate estimate of soil moisture. For instance, neutron count rates integrated over the entire day were used in a humid forest ecosystem located in the west of Germany, because hourly count rates were too low for accurate soil moisture measurements (Bogena et al., 2013). The results presented in our study show that care must be taken when integrating the cosmic-ray measurements over a longer period while combining with models, suggesting a potential trade-off between individual sensor accuracy and successful representation of soil moisture profile dynamics. This could imply in an "optimal range" for integration of neutron counts for a specific site location, but the investigation is beyond the scope of this study. For example, our initial preliminary analysis indicated little difference between the DA 2-day case with another assimilation case where neutron measurements were assimilated daily.

This study focused on the analysis using synthetic observations, mainly because (1) there is a lack of independent soil moisture observations corresponding to a similar effective horizontal area measured by the cosmic-ray sensor, and (2) the neutron intensity signal is entirely derived from soil moisture dynamics, which allows us to focus on the key aspects of the neutron–soil moisture interactions. Neither the COSMIC operator nor the Noah have explicitly dealt with additional sources of hydrogen (Franz et al., 2013a) other than the lattice water (explicitly described by a parameter in COSMIC; see Shuttleworth et al., 2013). Typical sources include surface water (Franz et al., 2012a), atmospheric water vapor (Rosolem et al., 2013), biomass (Franz et al., 2013b), and litter layer, soil organic matter and below-ground biomass (Bogena et al., 2013). For instance, changes in biomass over time may become important, especially at the Nebraska (cropland) site. However, as with any OSSE, there are some limitations in our approach because the uncertainties due to the above-mentioned sources of hydrogen are not introduced in the measurements. Furthermore, any potential structural deficiency in Noah when simulating soil moisture is ignored in this OSSE, hence model adjustments need not be applied to remove or reduce systematic biases (Draper et al., 2011; Kumar et al., 2012; Yilmaz and Crow, 2013). As a consequence, the results from this OSSE are likely to indicate better agreement relative to those obtained from assimilation of real neutron measurements. The assimilation of actual cosmic-ray neutron measurements will be investigated in the near future (e.g., http://www.bris.ac.uk/news/2014/august/soilmoistureand-cosmic-rays.html).

Finally, these results can also give some additional insights into applications of data assimilation to satellite remote-sensing products, whose measurements are provided globally at coarser temporal resolution. However, it is not the intention of the present study to directly compare the value of the cosmic-ray observations with more traditional satellite remote-sensing products, especially because their horizontal effective measurement areas are quite different (Robinson et al., 2008) and hence are likely to be influenced differently

by distinct factors (see Fig. 1 in Crow et al., 2012). Such analyses are beyond the scope of this study, but we encourage the use of cosmic-ray sensors in combination with satellite remote-sensing products for hydrometeorological applications because the information content from each measurement can be strongly linked to their individual dynamics.

The Supplement related to this article is available online at doi:10.5194/hess-18-4363-2014-supplement.

References

Anderson, J. L.: An ensemble adjustment Kalman filter for data assimilation, Mon. Weather Rev., 129, 2884–2903, 2001.

Anderson, J. L.: A local least squares framework for ensemble filtering, Mon. Weather Rev., 131, 634–642, 2003.

Anderson, J. L.: Exploring the need for localization in ensemble data assimilation using a hierarchical ensemble filter, Physica D: Nonlinear Phenomena, 230, 99–111, doi:10.1016/j.physd.2006.02.011, 2007.

Anderson, J. L.: Ensemble Kalman filters for large geophysical applications, IEEE Control Syst. Mag., 29, 66–82, doi:10.1109/MCS.2009.932222, 2009.

Anderson, J. L., Hoar, T., Raeder, K., Liu, H., Collins, N., Torn, R., and Avellano, A.: The Data Assimilation Research Testbed: A Community Facility, B. Am. Meteorol. Soc., 90, 1283–1296, doi:10.1175/2009BAMS2618.1, 2009.

Baker, I. T., Denning, A. S., Hanan, N., Prihodko, L., Uliasz, M., Vidale, P. L., Davis, K., and Bakwin, P.: Simulated and observed fluxes of sensible and latent heat and CO_2 at the WLEF-TV tower using SiB2. 5, Global Change Biol., 9, 1262–1277, 2003.

Baker, I. T., Prihodko, L., Denning, A. S., Goulden, M., Miller, S., and da Rocha, H. R.: Seasonal drought stress in the Amazon: Reconciling models and observations, J. Geophys. Res., 113, G00B01, doi:10.1029/2007JG000644, 2008.

Baldocchi, D. D.: Assessing the eddy covariance technique for evaluating carbon dioxide exchange rates of ecosystems: past, present and future, Global Change Biol., 9, 479–492, 2003.

Best, M. J., Pryor, M., Clark, D. B., Rooney, G. G., Essery, R .L. H., Ménard, C. B., Edwards, J. M., Hendry, M. A., Porson, A., Gedney, N., Mercado, L. M., Sitch, S., Blyth, E., Boucher, O.,

Cox, P. M., Grimmond, C. S. B., and Harding, R. J.: The Joint UK Land Environment Simulator (JULES), model description – Part 1: Energy and water fluxes, Geosci. Model Dev., 4, 677–699, doi:10.5194/gmd-4-677-2011, 2011.

Blunden, J. and Arndt, D. S.: State of the Climate in 2012, B. Am. Meteorol. Soc., 94, S1–S258, doi:10.1175/2013BAMSStateoftheClimate.2, 2013.

Bogena, H. R., Huisman, J. A., Baatz, R., Hendricks Franssen, H.-J., and Vereecken, H.: Accuracy of the cosmic-ray soil water content probe in humid forest ecosystems: The worst case scenario, Water Resour. Res., 49, 5778–5791, doi:10.1002/wrcr.20463, 2013.

Bonan, G. B., Oleson, K. W., Vertenstein, M., Levis, S., Zeng, X., Dai, Y., Dickinson, R. E., and Yang, Z. L.: The Land Surface Climatology of the Community Land Model Coupled to the NCAR Community Climate Model, J. Climate, 15, 3123–3149, 2002.

Brown, M. E., Escobar, V., Moran, S., Entekhabi, D., O'Neill, P. E., Njoku, E. G., Doorn, B., and Entin, J. K.: NASA's Soil Moisture Active Passive (SMAP) Mission and Opportunities for Applications Users, B. Am. Meteorol. Soc., 94, 1125–1128, doi:10.1175/BAMS-D-11-00049.1, 2013.

Chen, F. and Dudhia, J.: Coupling an advanced land surface-hydrology model with the Penn State-NCAR MM5 modeling system. Part I: Model implementation and sensitivity, Mon. Weather Rev., 129, 569–585, 2001.

Chen, F., Mitchell, K., Schaake, J., Xue, Y., Pan, H. L., Koren, V., Duan, Q. Y., Ek, M., and Betts, A.: Modeling of land surface evaporation by four schemes and comparison with FIFE observations, J. Geophys. Res., 101, 7251–7268, 1996.

Clark, D. B., Mercado, L. M., Sitch, S., Jones, C. D., Gedney, N., Best, M. J., Pryor, M., Rooney, G. G., Essery, R. L. H., Blyth, E., Boucher, O., Harding, R. J., Huntingford, C., and Cox, P. M.: The Joint UK Land Environment Simulator (JULES), model description – Part 2: Carbon fluxes and vegetation dynamics, Geosci. Model Dev., 4, 701–722, doi:10.5194/gmd-4-701-2011, 2011.

Clark, M. P., Rupp, D. E., Woods, R. A., Zheng, X., Ibbitt, R. P., Slater, A. G., Schmidt, J., and Uddstrom, M. J.: Hydrological data assimilation with the ensemble Kalman filter: Use of streamflow observations to update states in a distributed hydrological model, Adv. Water Resour., 31, 1309–1324, doi:10.1016/j.advwatres.2008.06.005, 2008.

Coumou, D. and Rahmstorf, S.: A decade of weather extremes, Nat. Clim. Change, 2, 1–6, doi:10.1038/nclimate1452, 2012.

Crow, W. T., Berg, A. A., Cosh, M. H., Loew, A., Mohanty, B. P., Panciera, R., de Rosnay, P., Ryu, D., and Walker, J. P.: Upscaling sparse ground-based soil moisture observations for the validation of coarse-resolution satellite soil moisture products, Rev. Geophys., 50, RG2002, doi:10.1029/2011RG000372, 2012.

Davis, K. J., Bakwin, P. S., Yi, C. X., Berger, B. W., Zhao, C. L., Teclaw, R. M., and Isebrands, J. G.: The annual cycles of CO_2 and H_2O exchange over a northern mixed forest as observed from a very tall tower, Global Change Biol., 9, 1278–1293, 2003.

Dee, D. P.: Bias and data assimilation, Q. J. Roy. Meteorol. Soc., 131, 3323–3343, doi:10.1256/qj.05.137, 2005.

Desilets, D. and Zreda, M.: Footprint diameter for a cosmic-ray soil moisture probe: Theory and Monte Carlo simulations, Water Resour. Res., 49, 3566–3575, 2013.

Draper, C. S., Mahfouf, J. F., Calvet, J. C., Martin, E., and Wagner, W.: Assimilation of ASCAT near-surface soil moisture into the

SIM hydrological model over France, Hydrol. Earth Syst. Sci., 15, 3829–3841, doi:10.5194/hess-15-3829-2011, 2011.

Draper, C. S., Reichle, R. H., De Lannoy, G. J. M., and Liu, Q.: Assimilation of passive and active microwave soil moisture retrievals, Geophys. Res. Lett., 39, L04401, doi:10.1029/2011GL050655, 2012.

Dunne, S. and Entekhabi, D.: An ensemble-based reanalysis approach to land data assimilation, Water Resour. Res., 41, W02013, doi:10.1029/2004WR003449, 2005.

Ek, M. B.: Implementation of Noah land surface model advances in the National Centers for Environmental Prediction operational mesoscale Eta model, J. Geophys. Res., 108, 8851, doi:10.1029/2002JD003296, 2003.

Entekhabi, D., Njoku, E. G., O'Neill, P. E., Kellogg, K. H., Crow, W. T., Edelstein, W. N., Entin, J. K., Goodman, S. D., Jackson, T. J., and Johnson, J.: The soil moisture active passive (SMAP) mission, Proc. IEEE, 98, 704–716, doi:10.1109/JPROC.2010.2043918, 2010.

Evensen, G.: Sequential data assimilation with a nonlinear quasi-geostrophic model using Monte Carlo methods to forecast error statistics, J. Geophys. Res., 99, 10–10, 1994.

Evensen, G.: The Ensemble Kalman Filter: theoretical formulation and practical implementation, Ocean Dynam., 53, 343–367, doi:10.1007/s10236-003-0036-9, 2003.

Famiglietti, J. S., Ryu, D., Berg, A. A., Rodell, M., and Jackson, T. J.: Field observations of soil moisture variability across scales, Water Resour. Res., 44, W01423, doi:10.1029/2006WR005804, 2008.

Franz, T. E., Zreda, M., Ferré, T. P. A., Rosolem, R., Zweck, C., Stillman, S., Zeng, X., and Shuttleworth, W. J.: Measurement depth of the cosmic ray soil moisture probe affected by hydrogen from various sources, Water Resour. Res., 48, W08515, doi:10.1029/2012WR011871, 2012a.

Franz, T. E., Zreda, M., Rosolem, R., and Ferré, T. P. A.: Field Validation of a Cosmic-Ray Neutron Sensor Using a Distributed Sensor Network, Vadose Zone J., 11, doi:10.2136/vzj2012.0046, 2012b.

Franz, T. E., Zreda, M., Rosolem, R., and Ferré, T. P. A.: A universal calibration function for determination of soil moisture with cosmic-ray neutrons, Hydrol. Earth Syst. Sci., 17, 453–460, doi:10.5194/hess-17-453-2013, 2013a.

Franz, T. E., Zreda, M., Rosolem, R., Hornbuckle, B. K., Irvin, S. L., Adams, H., Kolb, T. E., Zweck, C., and Shuttleworth, W. J.: Ecosystem-scale measurements of biomass water using cosmic ray neutrons, Geophys. Res. Lett., 40, 3929–3933, doi:10.1002/grl.50791, 2013b.

Hamill, T. M., Whitaker, J. S., and Snyder, C.: Distance-dependent filtering of background error covariance estimates in an ensemble Kalman filter, Mon. Weather Rev., 129, 2776–2790, 2001.

Han, X., Hendricks Franssen, H.-J., Rosolem, R., Jin, R., Li, X., and Vereecken, H.: Correction of systematic model forcing bias of CLM using assimilation of cosmic-ray neutrons and land surface temperature: a study in the Heihe catchment, China, Hydrol. Earth Syst. Sci. Discuss., 11, 9027–9066, doi:10.5194/hessd-11-9027-2014, 2014.

Hawdon, A., McJannet, D., and Wallace, J.: Calibration and correction procedures for cosmic-ray neutron soil moisture probes located across Australia, Water Resour. Res., 50, 5029–5043, doi:10.1002/2013WR015138, 2014.

Houtekamer, P. L. and Mitchell, H. L.: Data assimilation using an ensemble Kalman filter technique, Mon. Weather Rev., 126, 796–811, 1998.

IPCC: Summary for Policymakers, in: Managing the Risks of Extreme Events and Disasters to Advance Climate Change Adaptation, edited by: Field, C. B., Barros, V., Stocker, T. F., Qin, D., Dokken, D. J., Ebi, K. L., Mastrandrea, M.,D., Mach, K. J., Plattner, G.-K., Allen, S. K., Tignor, M., and Midgley, P. M., A Special Report of Working Groups I and II of the Intergovernmental Panel on Climate Change, Cambridge University Press, Cambridge, UK, and New York, NY, USA, 1–19, 2012.

Kalman, R. E.: A new approach to linear filtering and prediction problems, J. Basic Eng., 82, 35–45, 1960.

Kalman, R. E. and Bucy, R. S.: New results in linear filtering and prediction theory, J. Basic Eng., 83, 95–108, 1961.

Kerr, Y. H., Waldteufel, P., Wigneron, J.-P., Delwart, S., Cabot, F., Boutin, J., Escorihuela, M.-J., Font, J., Reul, N., Gruhier, C., Juglea, S. E., Drinkwater, M. R., Hahne, A., Martin-Neira, M., and Mecklenburg, S.: The SMOS Mission: New Tool for Monitoring Key Elements of the Global Water Cycle, Proc. IEEE, 98, 666–687, doi:10.1109/JPROC.2010.2043032, 2010.

Koster, R. D., Dirmeyer, P. A., Guo, Z., Bonan, G., Chan, E., Cox, P., Gordon, C. T., Kanae, S., Kowalczyk, E., and Lawrence, D.: Regions of strong coupling between soil moisture and precipitation, Science, 305, 1138–1140, 2004.

Kumar, S. V., Reichle, R. H., Peters-Lidard, C. D., Koster, R. D., Zhan, X., Crow, W. T., Eylander, J. B., and Houser, P. R.: A land surface data assimilation framework using the land information system: Description and applications, Adv. Water Resour., 31, 1419–1432, doi:10.1016/j.advwatres.2008.01.013, 2008.

Kumar, S. V., Reichle, R. H., Harrison, K. W., Peters-Lidard, C. D., Yatheendradas, S., and Santanello, J. A.: A comparison of methods for a priori bias correction in soil moisture data assimilation, Water Resour. Res., 48, W03515, doi:10.1029/2010WR010261, 2012.

Li, B., Toll, D., Zhan, X., and Cosgrove, B.: Improving estimated soil moisture fields through assimilation of AMSR-E soil moisture retrievals with an ensemble Kalman filter and a mass conservation constraint, Hydrol. Earth Syst. Sci., 16, 105–119, doi:10.5194/hess-16-105-2012, 2012.

Mackay, D. S., Ahl, D. E., Ewers, B. E., Gower, S. T., Burrows, S. N., Samanta, S., and Davis, K. J.: Effects of aggregated classifications of forest composition on estimates of evapotranspiration in a northern Wisconsin forest, Global Change Biol., 8, 1253–1265, 2002.

Margulis, S. A., McLaughlin, D., Entekhabi, D., and Dunne, S.: Land data assimilation and estimation of soil moisture using measurements from the Southern Great Plains 1997 Field Experiment, Water Resour. Res., 38, 35-1–35-18, doi:10.1029/2001WR001114, 2002.

McKay, M. D., Beckman, R. J., and Conover, W. J.: Comparison of three methods for selecting values of input variables in the analysis of output from a computer code, Technometrics, 21, 239–245, 1979.

Miller, J., Barlage, M., Zeng, X., Wei, H., Mitchell, K., and Tarpley, D.: Sensitivity of the NCEP/Noah land surface model to the MODIS green vegetation fraction data set, Geophys. Res. Lett., 33, L13404, doi:10.1029/2006GL026636, 2006.

Mitchell, K. E.: The multi-institution North American Land Data Assimilation System (NLDAS): Utilizing multiple GCIP products and partners in a continental distributed hydrological modeling system, J. Geophys. Res., 109, D07S90, doi:10.1029/2003JD003823, 2004.

Nearing, G. S., Crow, W. T., Thorp, K. R., Moran, M. S., Reichle, R. H., and Gupta, H. V.: Assimilating remote sensing observations of leaf area index and soil moisture for wheat yield estimates: An observing system simulation experiment, Water Resour. Res., 48, W05525, doi:10.1029/2011WR011420, 2012.

Niu, G.-Y., Yang, Z.-L., Mitchell, K. E., Chen, F., Ek, M. B., Barlage, M., Kumar, A., Manning, K., Niyogi, D., Rosero, E., Tewari, M., and Xia, Y.: The community Noah land surface model with multiparameterization options (Noah-MP): 1. Model description and evaluation with local-scale measurements, J. Geophys. Res., 116, D12109, doi:10.1029/2010JD015139, 2011.

Oleson, K. W., Niu, G. Y., Yang, Z. L., Lawrence, D. M., Thornton, P. E., Lawrence, P. J., Stöckli, R., Dickinson, R. E., Bonan, G. B., Levis, S., Dai, A., and Qian, T.: Improvements to the Community Land Model and their impact on the hydrological cycle, J. Geophys. Res., 113, G01021, doi:10.1029/2007JG000563, 2008.

Pitman, A. J.: The evolution of, and revolution in, land surface schemes designed for climate models, Int. J. Climatol., 23, 479–510, doi:10.1002/joc.893, 2003.

Reichle, R. H. and Koster, R. D.: Bias reduction in short records of satellite soil moisture, Geophys. Res. Lett., 31, L19501, doi:10.1029/2004GL020938, 2004.

Reichle, R. H., Walker, J. P., Koster, R. D., and Houser, P. R.: Extended versus ensemble Kalman filtering for land data assimilation, J. Hydrometeor, 3, 728–740, 2002.

Reichle, R. H., Koster, R. D., Liu, P., Mahanama, S. P. P., Njoku, E. G., and Owe, M.: Comparison and assimilation of global soil moisture retrievals from the Advanced Microwave Scanning Radiometer for the Earth Observing System (AMSR-E) and the Scanning Multichannel Microwave Radiometer (SMMR), J. Geophys. Res., 112, D09108, doi:10.1029/2006JD008033, 2007.

Reichle, R. H., Crow, W. T., and Keppenne, C. L.: An adaptive ensemble Kalman filter for soil moisture data assimilation, Water Resour. Res., 44, W03423, doi:10.1029/2007WR006357, 2008.

Robinson, D. A., Campbell, C. S., Hopmans, J. W., Hornbuckle, B. K., Jones, S. B., Knight, R., Ogden, F., Selker, J., and Wendroth, O.: Soil moisture measurement for ecological and hydrological watershed-scale observatories: A review, Vadose Zone J., 7, 358–389, 2008.

Rodell, M., Houser, P. R., Jambor, U., Gottschalck, J., Mitchell, K., Meng, C.-J., Arsenault, K., Cosgrove, B., Radakovich, J., Bosilovich, M., Entin, J. K., Walker, J. P., Lohmann, D., and Toll, D.: The Global Land Data Assimilation System, B. Am. Meteorol. Soc., 85, 381–394, doi:10.1175/BAMS-85-3-381, 2004.

Rosolem, R., Shuttleworth, W. J., Zeng, X., Saleska, S. R., and Huxman, T. E.: Land surface modeling inside the Biosphere 2 tropical rain forest biome, J. Geophys. Res., 115, G04035, doi:10.1029/2010JG001443, 2010.

Rosolem, R., Gupta, H. V., Shuttleworth, W. J., de Gonçalves, L. G. G., and Zeng, X.: Towards a comprehensive approach to parameter estimation in land surface parameterization schemes, Hydrol. Process., 27, 2075–2097, doi:10.1002/hyp.9362, 2012a.

Rosolem, R., Gupta, H. V., Shuttleworth, W. J., Zeng, X., and de Gonçalves, L. G. G.: A fully multiple-criteria implementation of the Sobol' method for parameter sensitivity analysis, J. Geophys. Res., 117, D07103, doi:10.1029/2011JD016355, 2012b.

Rosolem, R., Shuttleworth, W. J., Zreda, M., Franz, T. E., Zeng, X., and Kurc, S. A.: The Effect of Atmospheric Water Vapor on Neutron Count in the Cosmic-Ray Soil Moisture Observing System, J. Hydrometeor, 14, 1659–1671, doi:10.1175/JHM-D-12-0120.1, 2013.

Sabater, J. M., Jarlan, L., Calvet, J.-C., Bouyssel, F., and de Rosnay, P.: From Near-Surface to Root-Zone Soil Moisture Using Different Assimilation Techniques, J. Hydrometeor, 8, 194–206, doi:10.1175/JHM571.1, 2007.

Sakaguchi, K., Zeng, X., Christoffersen, B. J., Restrepo-Coupe, N., Saleska, S. R., and Brando, P. M.: Natural and drought scenarios in an east central Amazon forest: Fidelity of the Community Land Model 3.5 with three biogeochemical models, J. Geophys. Res., 116, G01029, doi:10.1029/2010JG001477, 2011.

Scott, R. L., Hamerlynck, E. P., Jenerette, G. D., Moran, M. S., and Barron-Gafford, G. A.: Carbon dioxide exchange in a semidesert grassland through drought-induced vegetation change, J. Geophys. Res., 115, G03026, doi:10.1029/2010JG001348, 2010.

Sellers, P. J., Shuttleworth, W. J., Dorman, J. L., Dalcher, A., and Roberts, J. M.: Calibrating the simple biosphere model for Amazonian tropical forest using field and remote sensing data. Part I: Average calibration with field data, J. Appl. Meteorol., 28, 727–759, 1989.

Sellers, P. J., Dickinson, R. E., Randall, D. A., Betts, A. K., Hall, F. G., Berry, J. A., Collatz, G. J., Denning, A. S., Mooney, H. A., and Nobre, C. A.: Modeling the exchanges of energy, water, and carbon between continents and the atmosphere, Science, 275, 502–509, 1997.

Seneviratne, S. I.: Climate science: Historical drought trends revisited, Nature, 491, 338–339, doi:10.1038/nclimate1633, 2012.

Seneviratne, S. I., Corti, T., Davin, E. L., Hirschi, M., Jaeger, E. B., Lehner, I., Orlowsky, B., and Teuling, A. J.: Investigating soil moisture–climate interactions in a changing climate: A review, Earth Sci. Rev., 99, 125–161, doi:10.1016/j.earscirev.2010.02.004, 2010.

Shuttleworth, J., Rosolem, R., Zreda, M., and Franz, T.: The COsmic-ray Soil Moisture Interaction Code (COSMIC) for use in data assimilation, Hydrol. Earth Syst. Sci., 17, 3205–3217, doi:10.5194/hess-17-3205-2013, 2013.

Teuling, A. J., Hirschi, M., Ohmura, A., Wild, M., Reichstein, M., Ciais, P., Buchmann, N., Ammann, C., Montagnani, L., and Richardson, A. D.: A regional perspective on trends in continental evaporation, Geophys. Res. Lett., 36, L02404, doi:10.1029/2008GL036584, 2009.

Topp, G. C., Davis, J. L., and Annan, A. P.: Electromagnetic Determination of Soil-Water Content – Measurements in Coaxial Transmission-Lines, Water Resour. Res., 16,, 574–582, 1980.

Verma, S. B., Dobermann, A., Cassman, K. G., Walters, D. T., Knops, J. M., Arkebauer, T. J., Suyker, A. E., Burba, G. G., Amos, B., Yang, H. S., Ginting, D., Hubbard, K. G., Gitelson, A. A., and Walter-Shea, E. A.: Annual carbon dioxide exchange in irrigated and rainfed maize-based agroecosystems, Agr. Forest Meteorol., 131, 77–96, doi:10.1016/j.agrformet.2005.05.003, 2005.

Walker, J. P. and Houser, P. R.: Requirements of a global near-surface soil moisture satellite mission: accuracy, repeat

time, and spatial resolution, Adv. Water Resour., 27, 785–801, doi:10.1016/j.advwatres.2004.05.006, 2004.

Wang, Z., Zeng, X., and Decker, M.: Improving snow processes in the Noah land model, J. Geophys. Res., 115, D20108, doi:10.1029/2009JD013761, 2010.

Western, A. W. and Blöschl, G.: On the spatial scaling of soil moisture, J. Hydrol., 217, 203–224, 1999.

Wikle, C. K. and Berliner, L. M.: A Bayesian tutorial for data assimilation, Physica D: Nonlinear Phenomena, 230, 1–16, doi:10.1016/j.physd.2006.09.017, 2007.

Wood, E. F., Roundy, J. K., Troy, T. J., van Beek, L. P. H., Bierkens, M. F. P., Blyth, E., de Roo, A., Döll, P., Ek, M., Famiglietti, J., Gochis, D., van de Giesen, N., Houser, P., Jaffé, P. R., Kollet, S., Lehner, B., Lettenmaier, D. P., Peters-Lidard, C., Sivapalan, M., Sheffield, J., Wade, A., and Whitehead, P.: Hyperresolution global land surface modeling: Meeting a grand challenge for monitoring Earth's terrestrial water, Water Resour. Res., 47, W05301, doi:10.1029/2010WR010090, 2011.

Yang, Z.-L., Niu, G.-Y., Mitchell, K. E., Chen, F., Ek, M. B., Barlage, M., Longuevergne, L., Manning, K., Niyogi, D., Tewari, M., and Xia, Y.: The community Noah land surface model with multiparameterization options (Noah-MP): 2. Evaluation over global river basins, J. Geophys. Res., 116, D12110, doi:10.1029/2010JD015140, 2011.

Yilmaz, M. T. and Crow, W. T.: The Optimality of Potential Rescaling Approaches in Land Data Assimilation, J. Hydrometeor., 14, 650–660, doi:10.1175/JHM-D-12-052.1, 2013.

Zacharias, S., Bogena, H., Samaniego, L., Mauder, M., Fuß, R., Pütz, T., Frenzel, M., Schwank, M., Baessler, C., Butterbach-Bahl, K., Bens, O., Borg, E., Brauer, A., Dietrich, P., Hajnsek, I., Helle, G., Kiese, R., Kunstmann, H., Klotz, S., Munch, J. C., Papen, H., Priesack, E., Schmid, H. P., Steinbrecher, R., Rosenbaum, U., Teutsch, G., and Vereecken, H.: A Network of Terrestrial Environmental Observatories in Germany, Vadose Zone J., 10, 955–973, doi:10.2136/vzj2010.0139, 2011.

Zhang, S.-W., Zeng, X., Zhang, W., and Barlage, M.: Revising the Ensemble-Based Kalman Filter Covariance for the Retrieval of Deep-Layer Soil Moisture, J. Hydrometeor., 11, 219–227, doi:10.1175/2009JHM1146.1, 2010.

Zhou, Y., McLaughlin, D., and Entekhabi, D.: Assessing the performance of the ensemble Kalman filter for land surface data assimilation, Mon. Weather Rev., 134, 2128–2142, 2006.

Zreda, M., Desilets, D., Ferré, T. P. A., and Scott, R. L.: Measuring soil moisture content non-invasively at intermediate spatial scale using cosmic-ray neutrons, Geophys. Res. Lett., 35, L21402, doi:10.1029/2008GL035655, 2008.

Zreda, M., Shuttleworth, W. J., Zeng, X., Zweck, C., Desilets, D., Franz, T., and Rosolem, R.: COSMOS: the COsmic-ray Soil Moisture Observing System, Hydrol. Earth Syst. Sci., 16, 4079–4099, doi:10.5194/hess-16-4079-2012, 2012.